Supplementary Information for

Protein Quantification using Controlled DNA Melting Transitions in Bivalent Probe Assemblies

*Joonyul Kim, Juan Hu, Andresa B. Bezerra, Mark D. Holtan, Jessica C. Brooks, and Christopher J. Easley**

Table of Contents

Experiment	Sequence name	Sequence (5'→3' with IDT codes); aptamer is underlined
Thrombin TFAB	Thr1_BFQ	CAG TCC GTG GTA GGG CAG GTT GGG GTG ACT TTT ACT TTC TGC ACG ACA CTT TGG AAC AGC /3IABkFQ/
	Thr2_TAMRA	/55-TAMK/ AAT AAC GTC AGA ATC GTA CTC GGG TGT GAC TAC TGG TTG GTG AGG TTG GGT AGT CAC AAA
	C9-12	GAC GTT ATT GCT GTT CCA AAG
	C8-12	AC GTT ATT GCT GTT CCA AAG
	C7-12	C GTT ATT GCT GTT CCA AAG
Insulin TFAB	AbA_BHQ2	/5AmMC6//iSp18/TCG TGG AAC TAT CTA GCG GTG TAC GTG AGT GGG CAT GTA GCA AGA GG/3BHQ_2/
	AbB_TYE665	/5TYE665/GTC ATC ATT CGA ATC GTA CTG CAA TCG GGT ATT AGG CTA /iSp18//3AmMC6T/
	AbA_BFQ	/5AmMC6//iSp18/TCG TGG AAC TAT CTA GCG GTG TAC GTG AGT GGG CAT GTA GCA AGA GG/3IABkFQ/
	AbB_TAMRA	/55-TAMK/ GTC ATC ATT CGA ATC GTA CTG CAA TCG GGT ATT AGG CTA /iSp18//3AmMC6T/
	C'10-10	G AAT GAT GAC CCT CTT GCT A
	C'10-8	AT GAT GAC CCT CTT GCT A
	C'10-7	T GAT GAC CCT CTT GCT A
Isothermal thrombin assay with a bivalent probe	Thr1_BFQ	CAG TCC GTG GTA GGG CAG GTT GGG GTG ACT TTT ACT TTC TGC ACG ACA CTT TGG AAC AGC/3IABkFQ/
	Thr2_TAMRA	/55-TAMK/A ATA ACG TCA GAA TCG TAC TCG GGT GTG ACT ACT GGT TGG TGA GGT TGG GTA GTC ACA AA
	C15-15	GAT TCT **U**AC GTT ATT GCT GTT CCA AAG **U**GT
	C8-12	AC GTT ATT GCT GTT CCA AAG

Table S-1. Single-stranded DNA (ssDNA) sequences used in this study. Strategically placed deoxyuridines in the C15-15 connector sequence permit enzymatic cleavage of the DNA strand by the Uracil DNA Excision Mix; deoxyuridines in the sequence are labeled with bold, blue text (**U**).

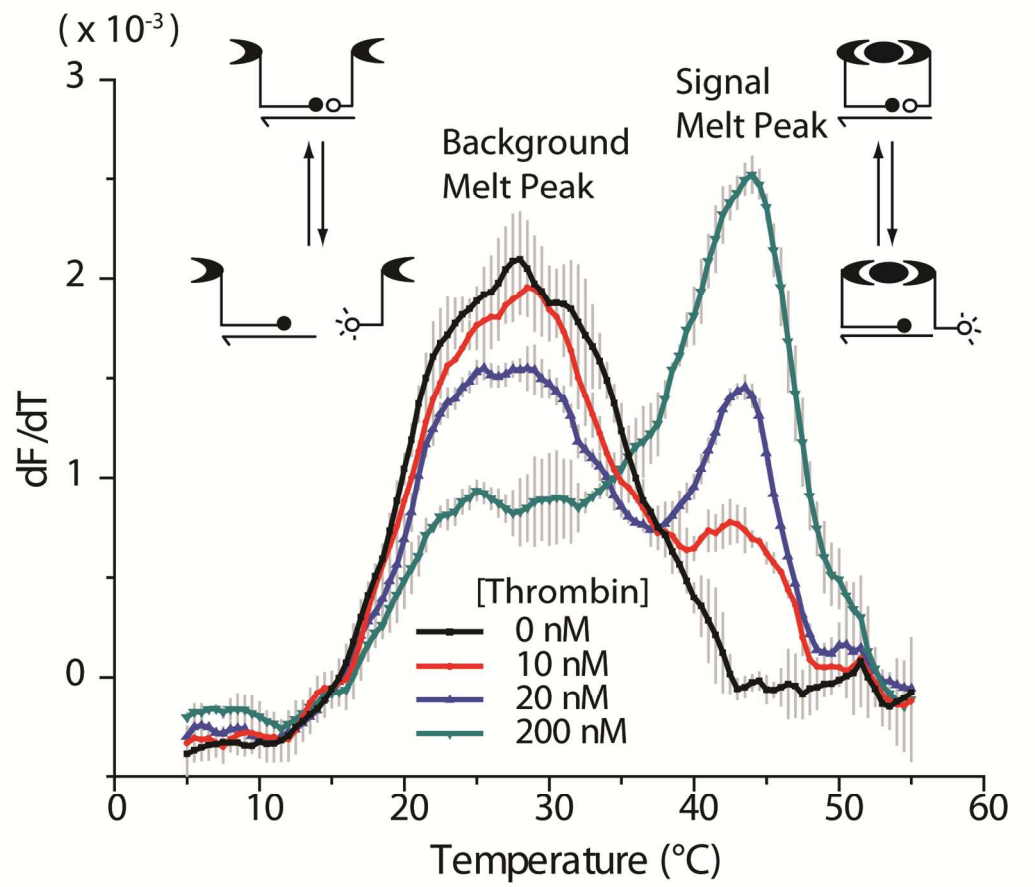

Figure S-1. Thrombin-dependent change in peak areas of background melt transition (BMT) and of signal melt transition (SMT).

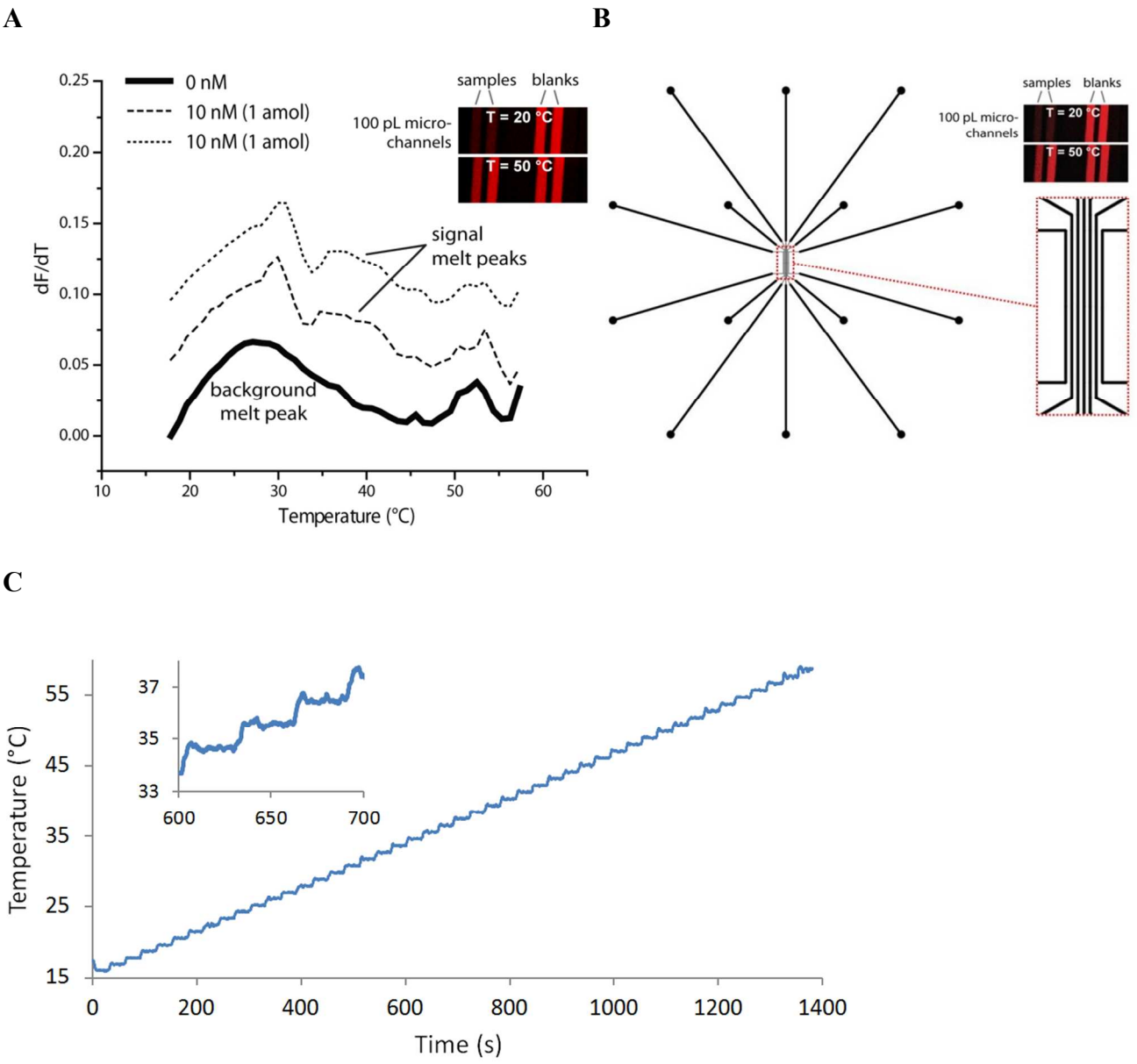

Figure S-2. Miniaturized TFAB for Thrombin detection (A) Assay performance. Miniaturization is straightforward, allowing direct fluorescence quantification of only 1 amol of Thrombin. (B) The photomask design. A seven-channel microfluidic device was designed specifically for small-volume fluorescence imaging (100 pL per channel in imaging region). Seven parallel channels, each 20 µm in width and 16 µm in depth at the imaging region (zoomed inset), were fabricated in polydimethylsiloxane (PDMS) using soft lithography [1]. Fluorescence emission (620 ± 30 nm) from microchannels was imaged with a Nikon Ti-E wide-field inverted fluorescence microscope with a 40x objective lens and an interrogated volume of 100 pL in each microchannel. (C) Characterization of the temperature control system during a typical run of microchip TFAB. The system was

designed utilizing a Maxim Integrated MAX1978 integrated controller for peltier modules, capable of delivering 2.2 A at up to 5 V. One 30 × 30 mm CP30138 peltier module (CUI Inc.), capable of sustaining a 66 °C temperature difference, was used to for the thermal pumping. The hot side of the peltier module was fitted with a 40 mm × 40 mm × 23 mm heat sink and a 30 mm × 30 mm fan capable of 3.72 ft^3 min^{-1} of airflow. The MAX1978 was driven with a LabVIEW application written in-house. The program integrates safety shutdown procedures, proportional integral derivative control, and data capture functionality. As shown in the inset data, once stabilized at the set temperature, the control system typically held the microfluidic device to within <0.2 °C of the set point. The temperature of the microchannels was increased from 15 °C to 60 °C in 1.0 °C increments, with 30 s hold times before fluorescence emission measurement (average of 2.0 °C min^{-1}). This temperature scanning was accomplished using an in-house built controller with a Peltier element driven by proportional-integral-derivative control (PID) provided by a LabVIEW application written in-house [2] [3].

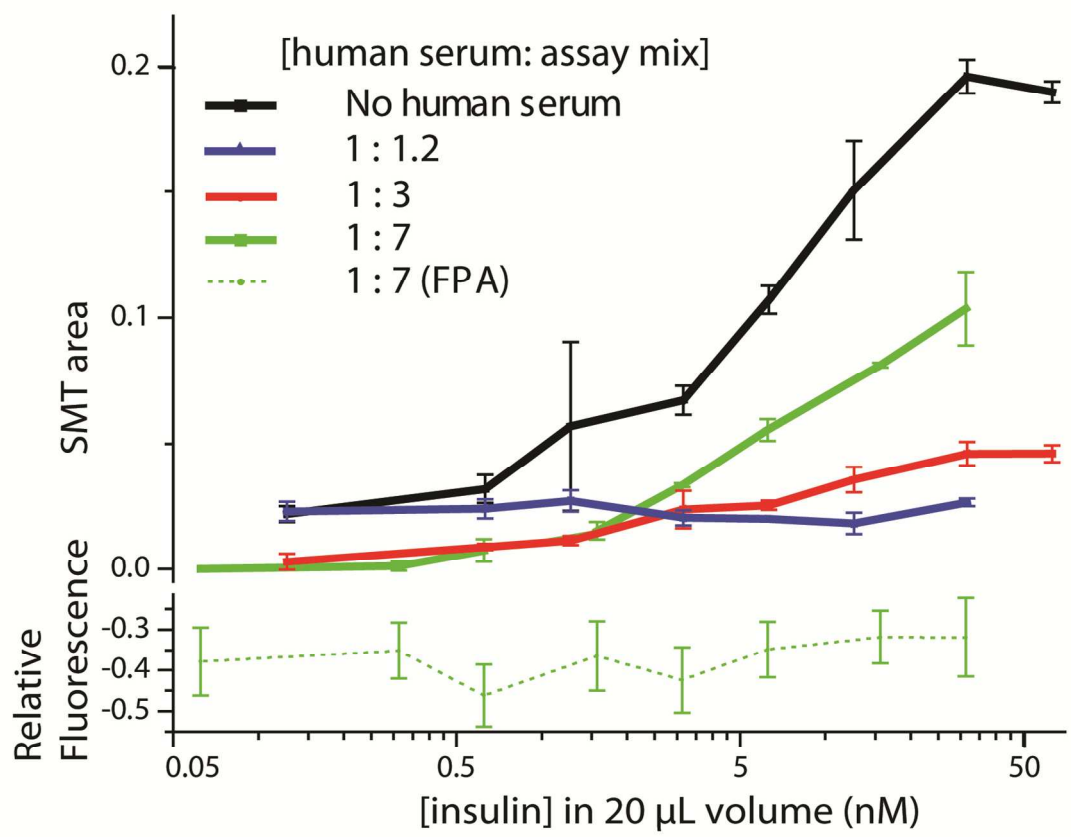

Figure S-3. Matrix effects on TFAB and isothermal fluorescence proximity assay (FPA). Insulin was spiked in samples containing various amount of human serum.

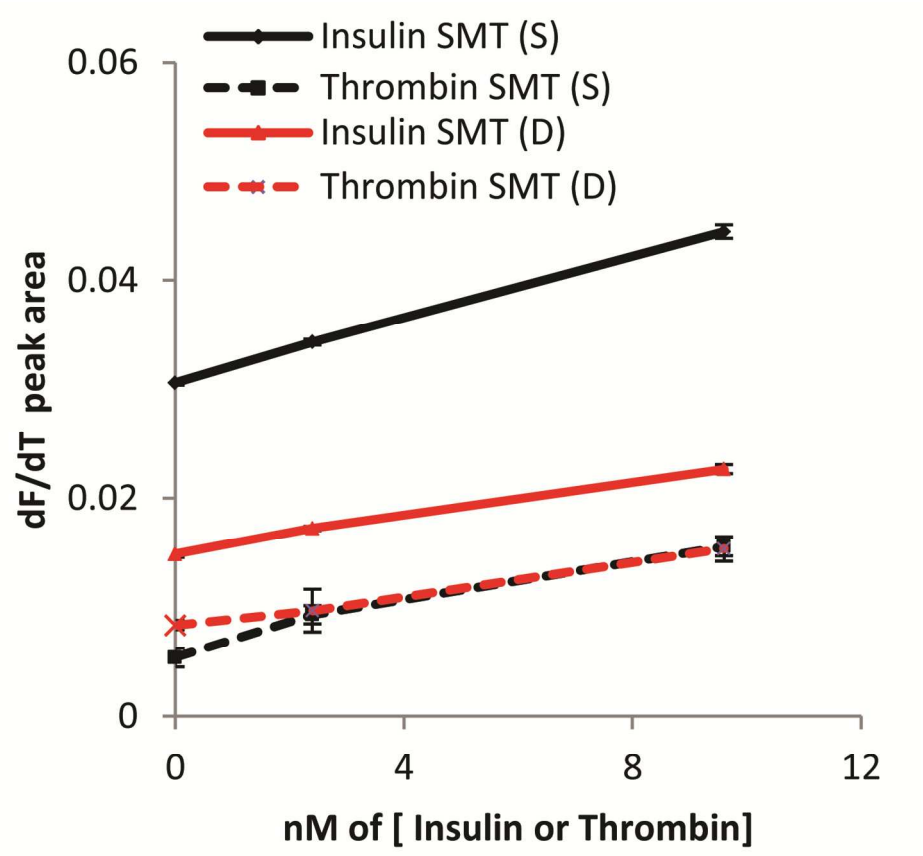

Figure S-4. Singleplex and duplex TFABs in 10-fold diluted serum samples for thrombin and insulin detection. The values in y-intercept are lower in thrombin assays, presumably due to well-separated background and signal melt peaks. The slopes representing assay sensitivity are slightly higher in duplex assay in both insulin and thrombin detection.

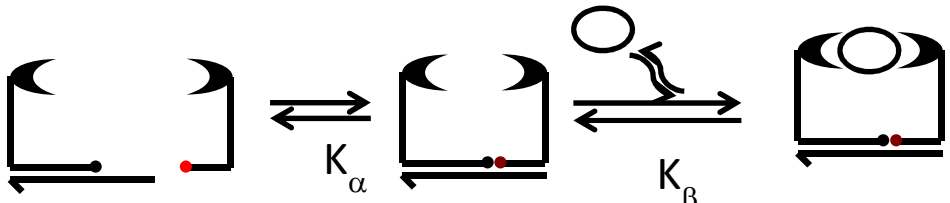

$$K_\alpha = \frac{[P1-Conn]\,[P2]}{[P1-P2-Conn]} \qquad K_\beta = \frac{[P1-P2-Conn][Target]}{[P1-P2-Conn-Target]}$$

During background melting

1. All targets are used up to make signal complex : $[P1-P2-Conn-Target] \cong [Target]_{total}$
2. Signal complexes are not dissociated : $\Delta\,[P1-P2-Conn-Target] \cong 0$

$$K_\alpha = \frac{[P1-Conn]\,[P2]}{[P1-P2-Conn]} = K_\alpha = \frac{[P2]^2}{[P2]_{total} - [P2] - [Target]_{total}}$$

During signal melting

1. All background complexes are dissociated : $[P1-P2-Conn] \cong 0$

$$K_\alpha\,K_\beta = \frac{[P1-Conn][P2][Target]}{[P1-P2-Conn-Target]} = \frac{[P2]^2([Target]_{total} - [P2]_{total} + [P2])}{[P2]_{total} - [P2]}$$

$$Ln\,(K) = \frac{\Delta S}{R} - \frac{\Delta H}{RT} \quad \text{(Van't Hoff plot)}$$

$$Ln\,(K_\alpha) = Ln\left(\frac{[P2]^2}{[P2]_t - [P2] - [Target]_t}\right) = -\frac{\Delta H_\alpha}{R}\left(\frac{1}{T}\right) + \frac{\Delta S_\alpha}{R}$$

$$Ln\,(K_\alpha K_\beta) = Ln\,(K_\alpha) + Ln(K_\beta) = Ln\left(\frac{[P2]^2\,([Target]_t - [P2]_t + [P2])}{[P2]_t - [P2]}\right)$$

$$Ln\,(K_\beta) = Ln\left(\frac{[P2]^2\,([Target]_t - [P2]_t + [P2])}{[P2]_t - [P2]}\right) - Ln(K_\alpha)$$

$$= -\frac{\Delta H_\beta}{R}\left(\frac{1}{T}\right) + \frac{\Delta S_\beta}{R}$$

$$= -\frac{\Delta H_\beta}{R}\left(\frac{1}{T}\right) + \frac{\Delta S_\beta}{R}$$

Figure S-5. The details on calculation of K_α and K_β formula.

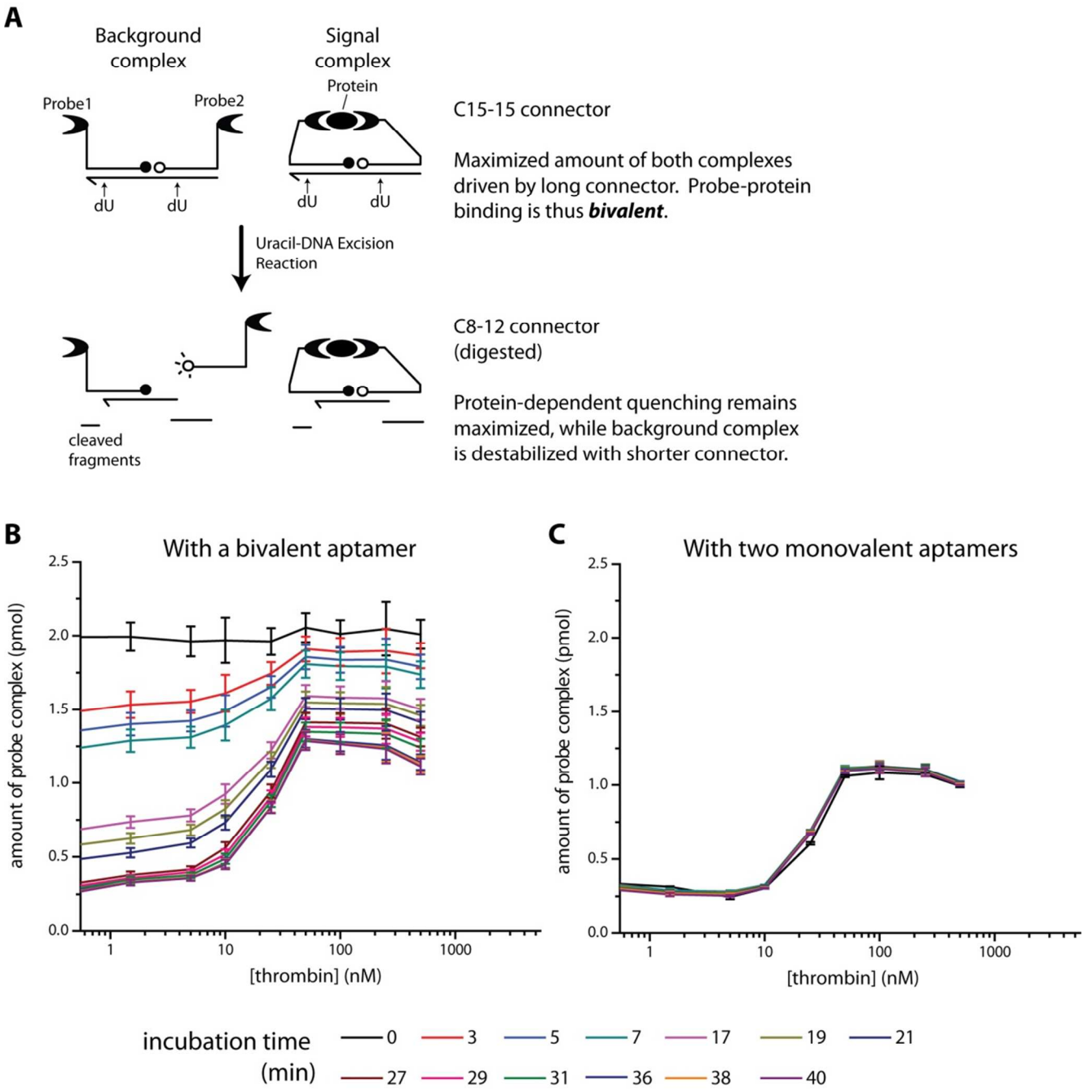

Figure S-6. **(A)** Schematic of isothermal bivalent fluorescence assay. **(B)** Conversion of C15-15 connector to C8-12 connector by the Uracil-DNA Excision Mix was monitored by thrombin FPA. As the reaction reached completion over ~30 min, background complexes were destabilized, while much of the signal complexes remained intact. This is evidenced by the emergence of protein-dependent signal over time. **(C)** By starting with the C8-12 connector (without bivalent probes), probe-target equilibrium had been established from the beginning of the excision reaction, thus there was no change over time, as expected.

Materials and Methods

Reagents and Materials. All solutions were prepared with deionized, ultra-filtered water (Fisher Scientific). The following reagents were used as received: insulin antibodies (clones 3A6 and 8E2; Fitzgerald Industries), bovine serum albumin (BSA), human thrombin and human insulin (Sigma-Aldrich), Uracil-DNA excision mixture (Epicentre), Amplitaq Gold DNA polymerase (Life Technologies), T4 DNA ligase (New England BioLab Inc.). Oligonucleotides were obtained from Integrated DNA Technologies (IDT; Coralville, Iowa), with purity and yield confirmed by mass spectrometry and HPLC, respectively. All DNA sequences used are given in Supporting Information Table S1; modifications included carboxytetramethylrhodamine (5-TAMRA; λ_{max}=546 nm; λ_{em}=579 nm), TYE665 (λ_{max}=645 nm; λ_{em}=665 nm), Blackhole Quencher-1 (BHQ1; λ_{max}=534 nm), and Blackhole Quencher-2 (BHQ2; λ_{max}=578 nm). DNA sequences were designed and optimized computationally using the nucleic acid package web server (NUPACK) [4]. Pathogen screened, normal human serum and plasma samples were purchased from Bioreclamation. The assay buffer consisted of 50 mM Tris-HCl at pH 7.5, 100 mM NaCl, 1 mM $MgCl_2$, and 1% BSA.

Preparation of probes. Thrombin aptamers (Thr1_BHQ1 and Thr2_TAMRA) were prepared by heating to 94 °C for 7 min, followed by rapid cooling on ice for 5 min in assay buffer. Antibody–oligonucleotide conjugates were prepared as described previously [5] by covalent attachment of AbA_BHQ1 to insulin antibody 3A6 (probe: 3A6_BHQ1) and AbB_TYE665 to insulin antibody 8E2 (probe: 8E2_TYE665), respectively. Conjugation and purification were accomplished using the Antibody-Oligonucleotide All-In-One Conjugation Kit (Solulink), according to the manufacturer's instructions. The final conjugate concentrations were determined via the BCA protein assay.

Thermofluorimetric analysis of bivalent probes (TFAB). For thrombin TFAB, the concentration of each component in a total of 20 µL assay buffer was as follows: 50 nM each of the pair of thrombin aptamers and 70 nM of DNA connector. For insulin TFAB in 20 µL assay buffer, concentrations were as follows: 6.3 nM each of the pair of insulin antibody-oligonucleotide conjugates and 18.9 nM of DNA connector. 5 µL of sample was used in both TFABs. The assay mixture was prepared at room temperature and stored at 4 °C until its use. After incubation of samples with assay mixture at 37°C for 15 min, the mixture was incubated either at 4 °C for additional 10 min for the full range of thermal scan (4 °C – 65 °C) or at 22 °C for additional 5 min for the short range of thermal scan (20 °C – 55 °C) before thermofluorimetric analysis. Fluorescence emission, either from

TAMRA (590 ± 20 nm) for thrombin TFAB or TYE665 (650 ± 40 nm) for insulin TFAB, was measured after reaching each targeted temperature. Isothermal fluorescence proximity assays (FPA) were performed at 22 °C.

Thermofluorimetric data analysis. Raw fluorescence emission data versus temperature was first corrected by subtracting data from a blank solution (assay buffer only) then normalized by the maximum, unquenched fluorescent probe (labeled DNA strands only, without quencher) over the entire temperature range. Derivative (dF/dT) plots were obtained using a first-derivative Savitzky-Golay filter in Microsoft Excel over a moving 5-point window. For quantitative analysis, dF/dT peaks (signal and background) were processed by nonlinear least squares fitting to the sum of two Gaussian peaks (Microsoft Excel, Solver add-in), with fixed mean peak temperatures defined by pilot experiments. These deconvoluted peak areas were referred to as "background melt peak area" (lower T_m) and "signal melt peak area" (higher T_m).

Microfluidic TFAB. Seven parallel microfluidic channels, each 20 μm in width and 16 μm in depth, were fabricated in polydimethylsiloxane (PDMS) using soft lithography [1]. The photomask design is given in Supplementary Information Figure S2. Fluorescence emission (620 ± 30 nm) from microchannels was imaged with a Nikon Ti-E wide-field inverted fluorescence microscope with a 40x objective lens and an interrogated volume of 100 pL in each microchannel. The temperature of the microchannels was increased from 15 °C to 60 °C in 1.0 °C increments, with 30 s hold times before fluorescence emission measurement (average of 2.0 °C min^{-1}). This temperature scanning was accomplished using an in-house built controller with a Peltier element driven by proportional-integral-derivative control (PID) provided by a LabVIEW application written in-house [2-3]. Thermal record data is shown in Supporting Information Figure S2.

Generation of two-dimensional thermofluorimetric maps The aptamer-based map for thrombin detection was collected by varying the temperature from 5 to 55 °C with a 0.5 °C interval and by varying protein concentration stepwise from 0 to 70 nM with a 5 nM interval. Heat maps (top to bottom) include background corrected the first derivative over temperature (dF/dT). Antibody-oligo based map for insulin detection from 0 to 6.5 nM in 0.5 nM increments. Thermofluorimetric maps were created using ImageJ. A two-dimensional text file of fluorescence intensity values (conc. as x-axis; T as y-axis) was imported as a Text Image and processed first with a two-pixel Gaussian blur filter. Partial derivative images were then created using 3 × 3 convolution filters; e.g. dF/dT matrix = {-1,-1,-1; 0,0,0; 1,1,1}. Images were finally scaled to a square aspect ratio and displayed using a "fire" lookup table for ease of visualization.

References

[1] G. M. Whitesides, E. Ostuni, S. Takayama, X. Jiang, D. E. Ingber, *Annual review of biomedical engineering* **2001**, *3*, 335-373.

[2] C. J. Easley, J. M. Karlinsey, J. M. Bienvenue, L. A. Legendre, M. G. Roper, S. H. Feldman, M. A. Hughes, E. L. Hewlett, T. J. Merkel, J. P. Ferrance, J. P. Landers, *Proceedings of the National Academy of Sciences of the United States of America* **2006**, *103*, 19272-19277.

[3] C. J. Easley, J. M. Karlinsey, J. P. Landers, *Lab on a chip* **2006**, *6*, 601-610.

[4] J. N. Zadeh, C. D. Steenberg, J. S. Bois, B. R. Wolfe, M. B. Pierce, A. R. Khan, R. M. Dirks, N. A. Pierce, *Journal of computational chemistry* **2011**, *32*, 170-173.

[5] C. J. DeJournette, J. Kim, H. Medlen, X. Li, L. J. Vincent, C. J. Easley, *Analytical chemistry* **2013**, *85*, 10556-10564.